Investigation of the Kinetics of Reduction of Iron Titanate ($FeTiO_3$) by Hydrogen

A. Kapilashrami, I. Arvanitidis and Du Sichen

Division of Theoretical Metallurgy
Royal Institute of Technology
S-100 44 Stockholm, Sweden

ABSTRACT

In the present study, the reduction kinetics of synthetic ilmenite by H_2 has been carried out using thermogravimetric technique. This has been complemented by X-ray diffraction and scanning electron microscopic (SEM) analyses. The morphology of the reduced product shows that iron metal is distributed around the titanium oxide particles, which has important implications for the separation of iron and titanium dioxide in the recovery of the same from ilmenite. The reduction proceeds very fast in the initial period and a high degree of reduction is obtained in the case of all reductions. A decrease in the reaction rate is observed at later stages of the reduction due to the slow diffusion process. An activation energy for the reduction of $FeTiO_3$ to iron and titanium dioxide was estimated to be of 108 $kJ \cdot mole^{-1}$.

I. INTRODUCTION

Among the titanium containing minerals, ilmenite ($FeTiO_3$) is the most abundant one in nature. The extraction of titanium from ilmenite ($FeTiO_3$) necessitates the initial separation of iron from the ores. Studies on the reduction of ilmenite ores have been made by a number of researchers /1-6/ in order to carry out the upgrading through pyrometallurgical routes. A number of reduction studies have used hydrogen gas as the reactant /3-6/. Since the kinetics of the reduction of ilmenite ores is strongly affected by the impurities present /7/, the results obtained in these earlier studies are specific to the ore types and the experimental conditions. In order to gain an insight into the reaction mechanism, it is necessary to study the reduction of synthetic $FeTiO_3$ by H_2 gas systematically. The kinetics and mechanism of reduction of synthetic ilmenite have been studied by several groups /5,8-10/. In all these investigations, densely compacted samples were employed. The use of dense compacts would involve a diffusion controlling or partially diffusion controlling mechanism. It has been proved /11-14/ that using shallow beds of fine oxide powder will allow the reductant gas to have access to all the particles in the sample and mass-transfer effects to be kept to a minimum. In the present work, very shallow powder beds are used so that the study can be focused on the chemical reactions, especially at the earlier stages.

Even from a theoretical viewpoint the reduction of ilmenite by hydrogen is of interest. The phase relationships in the Fe-Ti-O system are quite different below and above 1433 K due to the formation of the ferrous pseudobrookite $FeTi_2O_5$ /15,16/. It would be interesting to see the effect of this phase transformation on the reaction mechanism. Recently, kinetic studies of reduction of nickel, cobalt and iron tungstates by hydrogen have been carried out at this laboratory /11-13/. Comparison of the activation energies for the reduction of simple oxide and the tungstate in the case of iron, cobalt and nickel shows certain correlations between the activation energies for simple oxide and its corresponding tungstate. Studies of this aspect in the case of the titanates would throw light on the under-

standing of the correlations between the activation energies for reduction of simple oxides and the corresponding complex oxides with different complex anions. The present work is the first part of a series of studies on the reduction of transition metal titanate systems.

II. EXPERIMENTAL

A. Materials

Iron titanate powder (X-ray diffraction pattern conforms to standard pattern, 100 mesh, 37 wt% Fe(II)) was obtained from Aldrich, Steinheim, Germany. The hydrogen gas (SR grade) used for reduction and the argon gas (maximum of 2 ppm impurity) used during the pre-reduction period were supplied by AGA Gas, Stockholm.

B. Apparatus and procedure

The reduction studies were carried out in a SETARAM, TGA 92 (France) thermogravimetric unit having a detection limit of 1 μg. The equipment is fully controlled by an IBM PC through a CS92 controller. A detailed description of this apparatus has been given in an earlier publication /17/.

The experiments were carried out in the temperature range 923-1573 K. Powder samples of about 25 mg were employed in the present work. In a general run, the oxide powder bed was held in a shallow alumina crucible of 8 mm inside diameter and 2 mm in height. The crucible was hung by a Pt suspension wire in the thermobalance. The length of the Pt suspension wire was carefully adjusted to make sure that the powder bed was placed in the even temperature zone in the alumina reaction chamber. Before heating, the reaction tube was evacuated for 15 min down to a vacuum of 10 Pa. The tube was then filled with argon gas through the carrier gas inlet connected to the balance chamber. The sample was heated up in a constant argon flow of 0.05 l/min up to the reaction temperature. No weight change was observed during the heating period, indicating thereby that the moisture entrapment by the sample was negligible. After the stabilization of temperature, the reaction was started by arresting the argon gas flow and introducing hydrogen gas through an auxiliary gas inlet connected to the upper part of the reaction tube. The out-going gas was led out through the gas outlet at the lower part of the reaction chamber. A constant hydrogen flow rate of 0.7 l/min was then maintained during the whole course of the reduction. The weight changes of the sample were registered by a PC at intervals of 2 seconds. Preliminary experiments with different flow rates of H_2 showed that this flow rate was above the starvation rate, i.e. the resistance to the mass transfer in the gas phase was negligible compared to the chemical reaction and interdiffusion processes. The effect of the diffusion of either H_2 or H_2O through the powder bed on the reaction rate was investigated by repeating some experiments with different bed heights.

In order to have a better understanding of the reduction mechanism, X-ray diffraction and scanning electron microscopic (SEM) analyses of the partially and fully reduced samples were carried out. While powder samples were employed for the X-ray diffraction analyses, loosely compacted pellets of ilmenite were prepared for SEM analyses. The reactions were arrested at different stages by replacing H_2 gas with argon and cooling the samples at the maximum possible rate, viz 99 K/min. The samples were preserved in a desiccator before subjecting them to X-ray and SEM analyses. The X-ray diffraction studies were carried out on a X pert system (Philips). A scanning electron microscope, model Jeol JSM-840, connected with an EDS (Electron Dispersion Spectroscopy)-detector, Link AN-10000, was employed to study the microstructures of the samples and the chemical composition of the phases present.

III. RESULTS

The reduction curves at different temperatures up to 1487 K are presented in Figure 1. The dimensionless mass change, X, represents the ratio of the instant mass loss, ΔW_t to the theoretical mass loss, ΔW_∞, the latter corresponding to the loss of all the three oxygen atoms from $FeTiO_3$.

It is seen that the reaction proceeds very fast before a certain high X value has been reached in the case of all the experiments. Beyond this value, the reduction

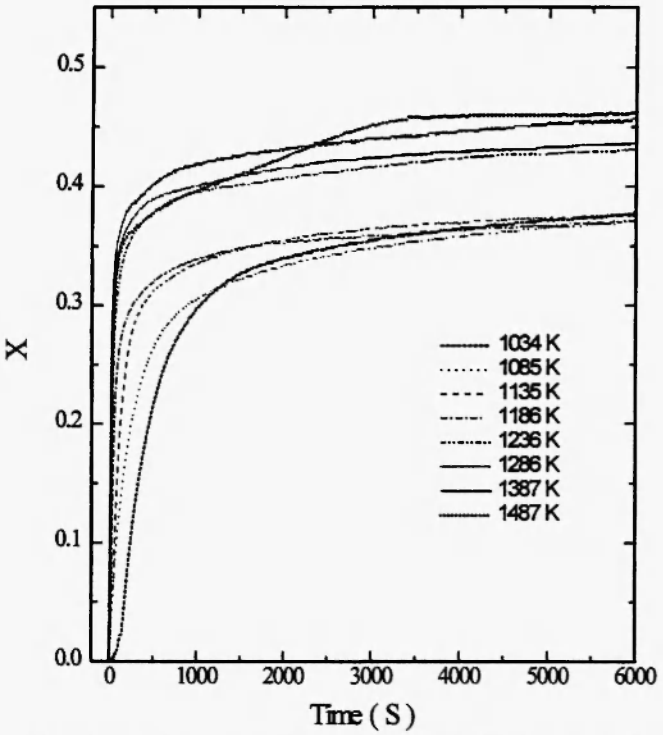

Fig. 1: The results of the reduction of $FeTiO_3$ at and below 1487 K.

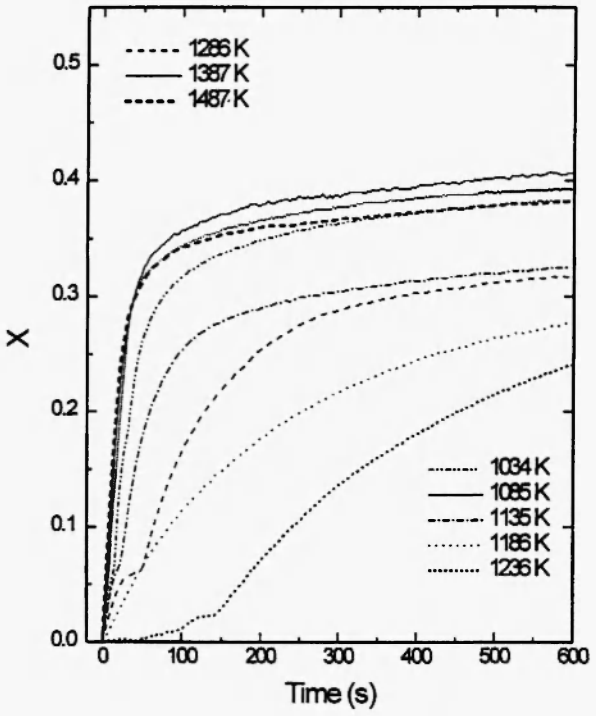

Fig. 2: The reduction curves of $FeTiO_3$ before 600 sec at and below 1487 K.

rate decreases dramatically and the reaction continues at a low rate for a very long time. The reduction curves are nearly horizontal after 6000 seconds, thus indicating that the reductions have almost reached the final stages. There is a common trend showing an increase in the X-value of the horizontal portion with the increasing reduction temperature. The reduction curves can be classified into three groups. The first group includes the reductions in the temperature range 1035-1186 K. These reductions come to a near-end around X = 0.35. The reduction curves of 1236 K, 1286 K and 1387 K belong to the second group showing an X value about 0.44 after 6000 seconds. The behaviour of the reduction at 1487 K differs from the first two groups. The reduction curve crosses the curves in the second group, reaching the highest degree of reduction at the final stages. In order to show the trends at the initial period of the reductions, the reduction curves before 600 seconds are enlarged in Figure 2. It is seen that the initial reaction rate increases with increasing temperature up to 1487 K.

The reduction curves at and above 1487 K are plotted in Figure 3. As shown in the Figure, a dramatic decrease in the reaction rate is observed in this temperature range. Visual examination of the samples after the experiments indicated the formation of a liquid phase during the reduction in the case of 1537 K and 1587 K. The presence of the liquid phase would reduce the reaction surface area, thereby leading to a decrease in the reaction rate.

Figure 4 presents the reduction curves for different bed heights at 1085 K. While the curves overlap at the initial stages, thereafter the reaction rate decreases with the increasing bed height. This indicates that, at the later stages of the reduction, the diffusion of either H_2 or H_2O through the powder bed plays an important role.

Based on their X-ray spectra, Bardi /4/ suggests that the reduction of ilmenite by hydrogen gas produces Fe and TiO_2 at 1123 K. In order to confirm this aspect, X-ray and SEM analyses were carried out for the partially and nearly completed reduced samples at 1085 K. Figures 5 and 6 present the photomicrographs of the

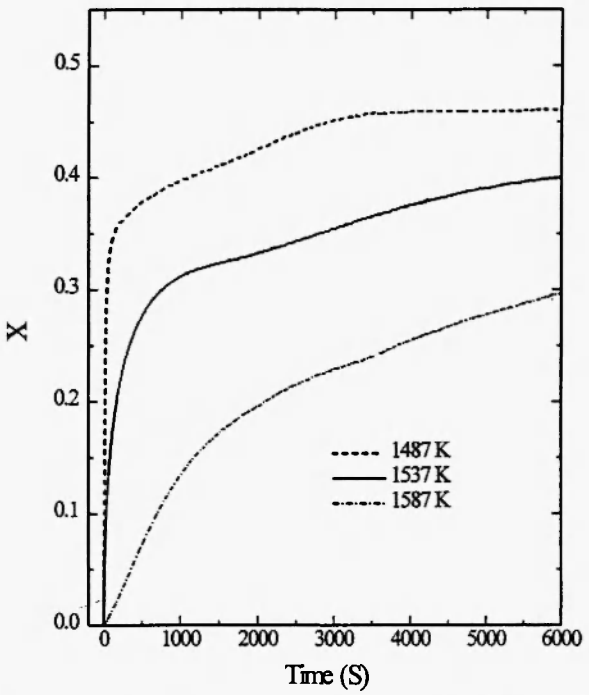

Fig. 3: The results of the reduction of $FeTiO_3$ at and above 1487 K.

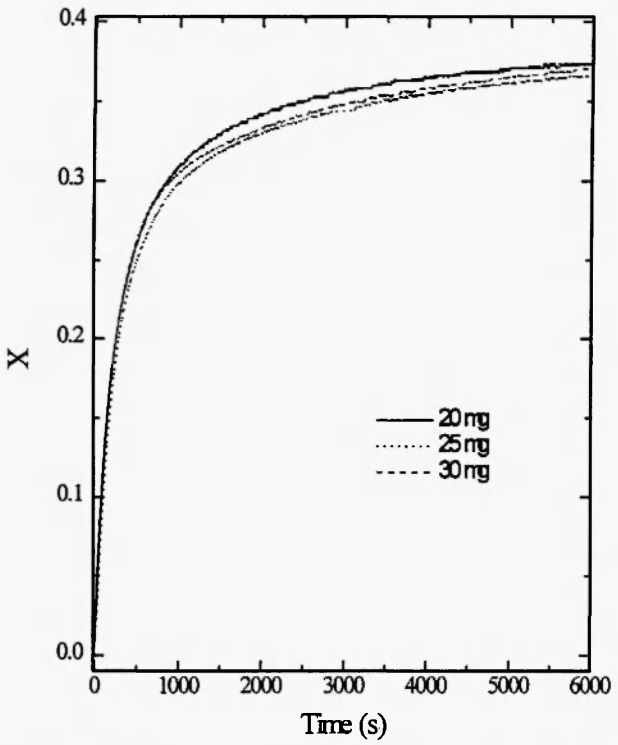

Fig. 4: The effect of the bed height on the reduction of $FeTiO_3$ at 1085 K.

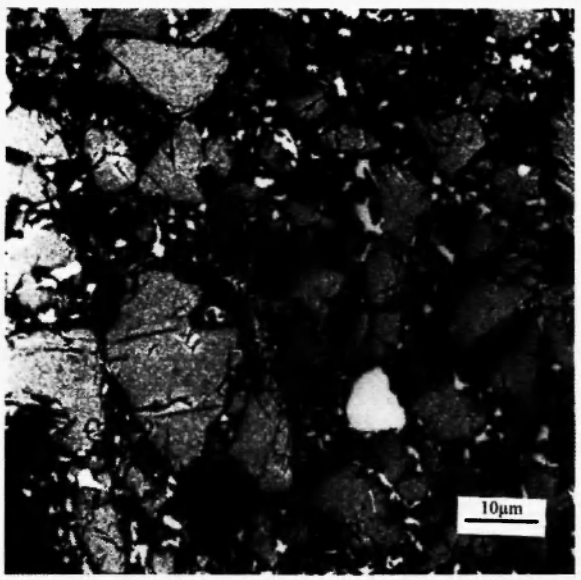

Fig. 5: The photomicrograph of the partially reduced $FeTiO_3$ sample (X = 0.13, 1085 K).

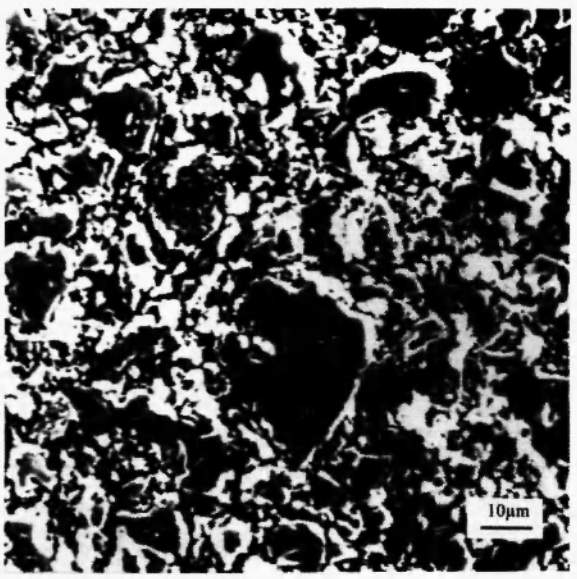

Fig. 6: The photomicrograph of the nearly completed reduced $FeTiO_3$ sample (X = 0.344, 1085 K).

reduced samples arrested at X = 0.13 and X = 0.344, respectively. Three phases coexist in the sample arrested at X = 0.13. According to the EDS analyses, the light phase is iron with a very small amount of titanium dissolved, the light grey phase is $FeTiO_3$ and the dark grey is TiO_2. Only two phases could be identified in the sample arrested at X = 0.344. As shown in Figure 6, the dark grey TiO_2 is surrounded by the light phase of iron with about 2-3 atom percent dissolved titanium. The existence of the above mentioned phases in the two samples was further confirmed by X-ray diffraction analyses. The peaks for the iron phase were found to be slightly shifted from those for the pure metal due to the dissolution of titanium. This is in conformity with the results of the SEM analyses.

IV. DISCUSSION

The isothermal sections of the Fe-Ti-O phase diagram at 1273 K and 1473 K suggested by Merritt and Turnbull /16/ are reproduced in Figure 7. Similar phase relationships at low oxygen potentials, which are relevant to the present work, have been reported by Borowiec and Rosenqvist /18/. From a thermodynamic viewpoint, $FeTiO_3$ will be reduced to TiO_2 and Fe in one step at temperatures lower than T = 1473 K. This reaction can be expressed as:

$$FeTiO_3(S) + H_2\ (G) = Fe(S) + TiO_2(S) + H_2O(g) \quad (1)$$

As mentioned in the Results section, the SEM analyses and the X-ray diffraction showed that while the sample arrested at X = 0.13 from 1085 K consisted of Fe, $FeTiO_3$ and TiO_2, the nearly completely reduced sample contained only Fe and TiO_2. This is in conformity to the one-step reaction route. The absence of Ti_3O_5 in the reduced samples suggests that TiO_2 cannot be further reduced at this temperature under these experimental conditions. It is seen in Figure 1 that the reductions below 1236 K almost finish around X = 0.35, which is slightly higher than the value X = 0.333 corresponding to the completion of the reaction (1). It is reasonable to conclude that the reductions below 1236 K proceed according to reaction (1). The

Fe–Ti–O

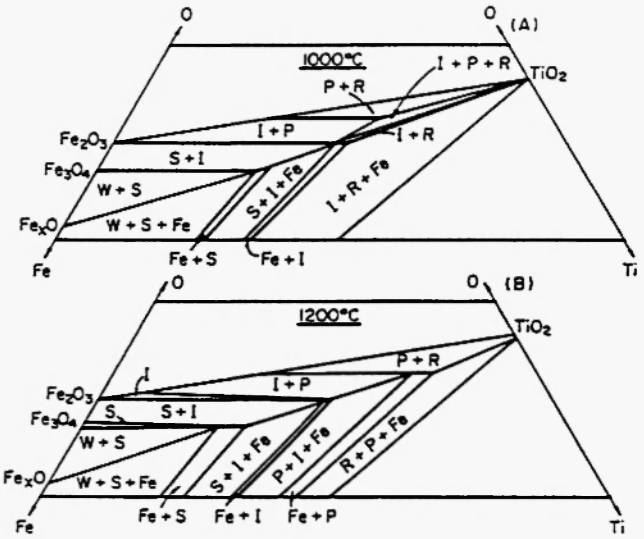

Fig. 7: Isothermal sections from the Fe-Ti-O phase diagram at 1273 and 1473 K /16/.
R: Rutile (TiO_2), W: Wustite ($Fe_{1-x}O$), I: ilmenite ($FeTiO_3$), P: pseudobrookite ($FeTi_2O_5$), S: spinal (Fe_2 (Fe,Ti)O_4)

slightly higher X values at the final stages of these reductions could be attributed to a slight reduction of TiO_2 and consequent solubility of titanium in iron. The phase diagram /19/ of the Fe-Ti system in Figure 8 indicates that α(Fe) has a solubility of about 3 atom percent Ti at 1073 K and the solubility increases with the increase of temperature. The dissolution of titanium in iron during the reduction was even confirmed by the results of X-ray diffraction and SEM analyses which showed that the produced iron contains 2-3 atom percent titanium.

As shown in Figure 1, the reduction curves in the second group (1236 K, 1286 K and 1387 K) have X values greater than 0.43 at the final stages. The degree of reduction increases with increasing reaction temperature in this group. Based on the X-ray diffraction results, Bardi /4/ reported that the reduction of $FeTiO_3$ by hydrogen gas at 1373 K resulted in iron and Ti_3O_5. No TiO_2 was detected in the reduced sample by the author. This is in accordance with the reaction curves present in the second group. The product of Ti_3O_5 suggests that in addition to reaction (1) the following

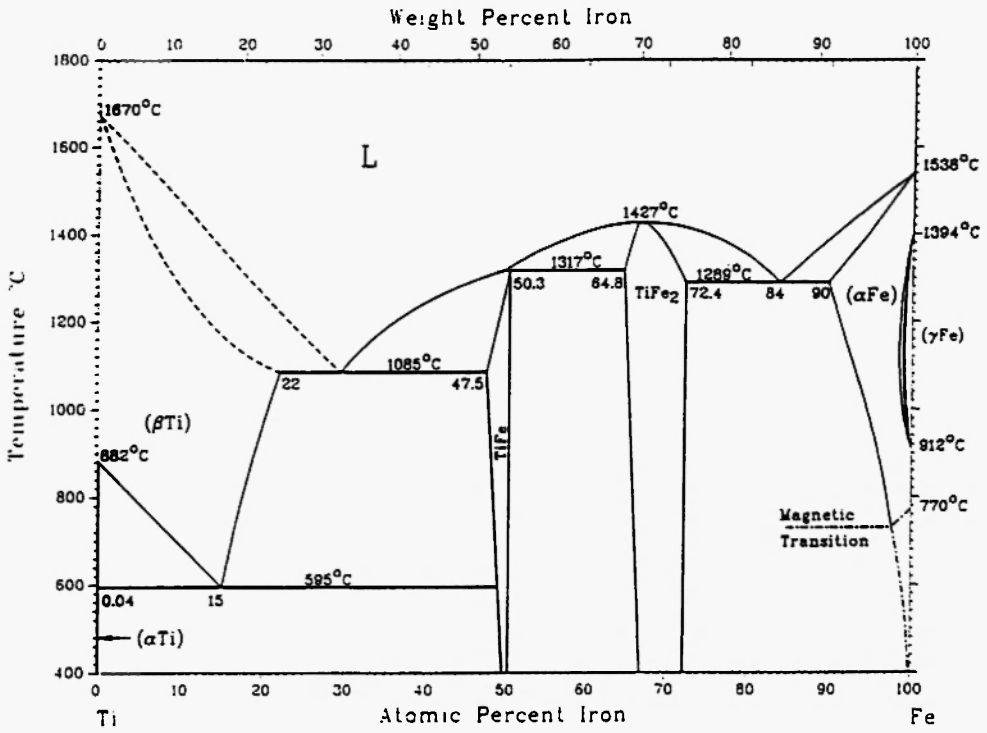

Fig. 8: Phase diagram of the Fe-Ti system /19/.

reaction would take place:

$$3TiO_2(S) + H_2(g) = Ti_3O_5(S) + H_2O(g) \quad (2)$$

The overall reaction can be expressed as:

$$\frac{3}{4}FeTiO_3(S) + H_2(G) = \frac{3}{4}Fe(S) + \frac{1}{4}Ti_3O_5(S) + H_2O(g) \quad (3)$$

On completion, reaction (3) leads to a degree of reduction of X = 0.444, which is very close to the final X values of the reductions in the second group. The excess weight loss of the reductions could once again be explained by the solubility of titanium in α(Fe), and the increasing final weight loss by the increase of the solubility with temperature. In their study of the reduction of ilmenite flake at 1287 K, Zhao and Shadman /9/ found that the reduction of TiO_2 did not occur to any significant extent before the completion of the iron metallization. They attributed this to the inhibition effect of water vapour as the reaction product. In the present work, powder sample was used and the bed height was only 0.5 mm. Hence the inhibition effect of water vapour would not be as serious as in the reduction carried out by Zhao and Shadman. The reduction curves in group 2 do not show any discontinuity in the slope, indicating thereby that the two-step reaction mechanism suggested by Zhao and Shadman /9/ would not be valid under the present experimental conditions. There may possibly be a period of gradual transition from reaction (1) to reaction (2) before the completion of the reduction of $FeTiO_3$ to Fe and TiO_2.

As seen in Figures 1 and 2, the reduction at 1487 K had the highest reaction rate at the initial stages. Thereafter the reaction rate decreased faster than the reductions in the second group. The reduction curve crosses the curves in the second group again since the reduction had a higher X value at the final stages compared to the rest of the reductions. The lower reaction rate at 1487 K after the initial stages could be attributed to the formation of the ferrous pseudo-brookite $FeTi_2O_5$. According to the isothermal section of the Fe-Ti-O system at 1473 K (Figure 7), the reduction path would, from a thermodynamic

standpoint, go through the three-phase equilibrium $FeTiO_3$–Fe–$FeTi_2O_5$, before the sample was reduced to the mixture of TiO_2-Fe and finally Ti_3O_5-Fe. The reduction curve at 1487 K in Figure 1 does not seem to suggest any dramatic change in the reduction process. However, the reduction of $FeTiO_3$ to Fe and TiO_2 might possibly need to go through a transition stage forming $FeTi_2O_5$, viz.

$$2FeTiO_3(S) + H_2(G) = FeTi_2O_5(S) + Fe(S) + H_2O(g) \quad (4)$$

It might also be possible that the titanium dioxide produced in reaction (1) would react with $FeTiO_3$ forming $FeTi_2O_5$ according to the following reaction:

$$FeTiO_3 + TiO_2 = FeTi_2O_5 \quad (5)$$

The total result of reactions (1) and (5) would be reaction (4). The multi-step chemical reaction process could proceed at a lower reaction rate. It should be pointed out that even reaction (2) would take place at the same time during the reduction process.

It is seen in Figure 5 that the light iron phase occurs only at the edges of the original ilmenite grains. The distribution of the dark grey TiO_2 in the light grey $FeTiO_3$ does not suggest a topochemical process. The photomicrograph of the nearly completely reduced sample in Figure 6 shows that the dark grey TiO_2 is surrounded by iron. The segregation of the product, viz. iron and titanium dioxide, indicates that iron diffuses out of the grain particles through the TiO_2 layer during the reduction. It could be expected that as the reduction proceeds, the diffusion distance for iron would increase and become more and more important in the reaction process. Thus, the diffusion of Fe would become the controlling step at the later stages of the reduction, which would explain why the reaction rate decreased dramatically after a certain X value and the reaction continued at a low rate for a very long time as shown in Figure 1.

As discussed in the Results section, even the diffusion of H_2O and H_2 through the powder bed could play an important role during the later stages of the reduction. The lack of information on both the diffusion constants of iron through the TiO_2 layer and hydrogen gas through the powder bed makes it difficult to employ the shrinking core model to evaluate the activation energy of reaction (1) using the reduction data. On the other hand, the bed height does not have a significant effect on the reduction rate at the earlier stages of the reduction as shown in Figure 4. Since a very small particle size (4 μm) was employed in the present work, the diffusion distance of iron through TiO_2 would be very short at the initial stages so that the resistance to the diffusion is also negligible in this period. It could thus be expected that the reduction rate was controlled by the chemical reaction in the initial reaction period. From the rates of the reaction obtained at the initial stages for the reductions in the first group (1034-1186 K), the activation energy for reaction (1) could be calculated using Arrhenius plots. Such a plot is given in Fig. 9. In order to avoid experimental errors due to the transient hydrogen partial pressure when Ar is replaced by H_2, the reduction rate for each reduction was taken at the point when the rate was maximum.

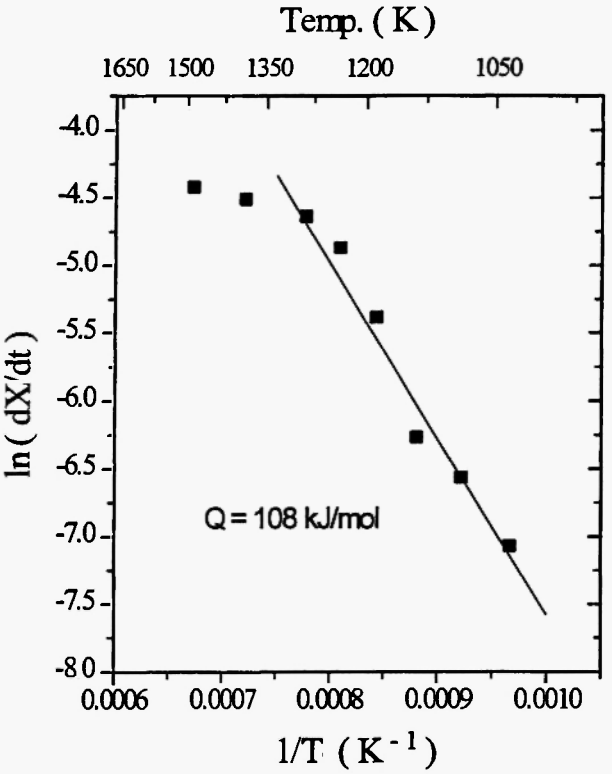

Fig. 9: Arrhenius plot for the reduction of $FeTiO_3$

It usually took a few seconds for the reaction rates to show the maximum. The linear regression in Figure 9 reveals an activation energy of 108 $kJ.mol^{-1}$. The reaction rates, in the natural logarithmic form, obtained for the other reductions are also included in this Figure. Since reaction (2), in the case of group 2, and reactions (2) and (3), in the case of the reduction at 1487 K, could take place at the same time as reaction (1) and complicate the reduction process, these data were not employed in the calculation of the activation energy. However, it is interesting to see that the points obtained at 1236 K and 1286 K fall on the regression line, thus indicating that reaction (2) did not have an appreciable effect on the reaction rate at these temperatures. The point corresponding to the reduction at 1386 K in the second group is below the regression line. The lower reaction rate might be due to the increasing contribution of reaction (2). Similarly the lower reaction rate at 1487 K regarding the regression could be attributed to the multi-step chemical reaction involving reactions (1), (2) and (4) at this temperature. It should be pointed out that at and above 1387 K, the initial reaction rate is very high. It is also possible that the transient hydrogen partial pressure had introduced experimental uncertainties in these experiments. The lower reactions rates could even be due to the sintering effect, which would reduce the area of the reaction surface and thus decrease the reaction rate to some extent. The calculated activation energy in the temperature range 1034-1186 K can be compared with the values reported by Zhao and Shadman /9/ as well as Briggs and Sacco /10/. While the former authors used flakes of synthetic ilmenite in their study, the latter employed synthetic ilmenite disks. A value of 93 $kJ.mole^{-1}$ was obtained by Zhao and Shadman /9/ using the initial reaction rates of the reduction. On the other hand, Briggs and Sacco /10/ evaluated an activation energy of 180 $kJ{\cdot}mole^{-1}$ using a shrinking core model. The present result is in fair agreement with that of Zhao and Shadman and is much lower than the value by Briggs and Sacco /10/.

As shown in Figure 5, the reduction of ilmenite by hydrogen at 1085 K leads to the complete separation of iron from the titanium dioxide particles. The segregation of iron and TiO_2 has important implications for the separation of iron and titanium dioxide in the recovery of the same from ilmenite. In order to separate iron from titanium, ilmenite ore could be reduced by hydrogen gas at a temperature around 1073 K. This could be followed by smelting, whereby liquid iron is formed and removed. Even a magnetic separation between the reduction and smelting could be considered, by which a great portion of metallic iron could be removed from the oxide. At temperatures higher than 1186 K, TiO_2 will be reduced to Ti_3O_5. The reduction above 1537 K will result in the formation of a liquid phase, leading to poor kinetic conditions for the reduction.

V. SUMMARY AND CONCLUSION

In the present work, the reduction of $FeTiO_3$ was investigated by a thermogravimetric method. Shallow powder beds were employed in order to allow the reductant gas to have access to all particles thereby minimising the mass-transfer effects and emphasizing the chemical reaction. The reaction proceeds very fast before a high degree of reduction has been reached in the case of all the experiments. The reduction rate decreases dramatically at the later stages of the reduction and the reaction continues at a low rate for a very long time. Below 1186 K, ilmenite is reduced to TiO_2 and iron. At and above this temperature, the reduction products are found to be iron and Ti_3O_5. The activation energy of the reduction of $FeTiO_3$ to TiO_2 and iron has been calculated to be 108 $kJ{\cdot}mole^{-1}$ using the reaction rates obtained at the initial stages of the reductions.

ACKNOWLEDGEMENTS

The authors wish to thank Professor S. Seetharaman for his valuable advice and for the help received during the preparation of this paper. Financial support for this work from the Swedish Council for Technical Sciences (TFR) is gratefully acknowledged.

REFERENCES

1. R. Merk and C.A. Pickles, *Canad. Metall. Quarterly,* **27**, 179-185 (1988).
2. I.E. Grey, A.F. Reid and D.G. Jones, *Trans. Inst. Min. Metall.*, **83**, 39 (1974).
3. D.G. Jones, *J. Appl. Chem. Biotechnol.*, **25**, 561 (1975).
4. D. Bardi, *Mater. Chem. & Phys.*, **17**, 325-341 (1987).
5. K. Sun, R. Takahashi and J. Yagi, *ISIJ International,* **32**, 496-504 (1992).
6. K. Sun, T. Akiyama, R. Takahashi and J. Yagi, *ISIJ International,* **35**, 360-366 (1995).
7. I.E. Grey, A.F. Reid and D.G. Jones, *Trans. Inst. Min. Metall.*, **83**, 105 (1974).
8. K. Sun, R. Takahashi and J. Yagi, *ISIJ International,* **33**, 523-528 (1993).
9. Y. Zhao and F. Shadman, *Ind. Eng. Chem. Res.*, **30**, 2080-2087 (1991).
10. R.A. Briggs and A. Sacco, Jr., *J. Mater. Res.*, **6**, 574-584 (1991).
11. S. Sridhar, Du Sichen and S. Seetharaman, *Z. Metallkunde,* **85**, 616-620 (1994).
12. S. Sridhar, Du Sichen and S. Seetharaman, *Metall-Material Trans.*, **25B**, 391-396 (1994).
13. J.A. Bustnes, Du Sichen and S. Seetharaman, *Metall-Material Trans.*, **26B**, 547-552 (1995).
14. J.A. Bustnes, Du Sichen and S. Seetharaman, "Design fundamentals of composites, intermetallics and metal/ceramic systems", *TMS Annual Meeting*, 1996.
15. S. Akimoto, T. Nagata and T. Katsura, *Nature, Lond.*, **179**, 37 (1957).
16. P.R. Merritt and A.G. Turnbull, *J. Solid State Chem.*, **10**, 252-259 (1974).
17. Du Sichen and S. Seetharaman, *Metall. Trans.*, **23B**, 317-324 (1992).
18. K. Borowiec and T. Rosenqvist, *Scand. J. Metall.*, **10**, 217-224 (1981).
19. J.L. Murray, *Bulletin of Alloy Phase Diagram,* **2**, 320-334 (1981).